Article

Effect of Subsurface Oxygen on the Reactivity of the Ag(111) Surface

Ye Xu, Jeff Greeley, and Manos Mavrikakis

J. Am. Chem. Soc., **2005**, 127 (37), 12823-12827• DOI: 10.1021/ja043727m • Publication Date (Web): 27 August 2005

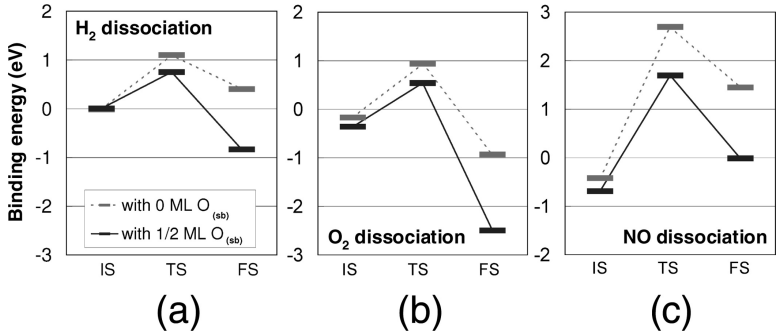

More About This Article

Additional resources and features associated with this article are available within the HTML version:

- Supporting Information
- Links to the 15 articles that cite this article, as of the time of this article download
- Access to high resolution figures
- Links to articles and content related to this article
- Copyright permission to reproduce figures and/or text from this article

View the Full Text HTML

J|A|C|S
ARTICLES
Published on Web 08/27/2005

Effect of Subsurface Oxygen on the Reactivity of the Ag(111) Surface

Ye Xu, Jeff Greeley, and Manos Mavrikakis*

Contribution from the Department of Chemical and Biological Engineering, University of Wisconsin—Madison, Madison, Wisconsin 53706

Received October 14, 2004; E-mail: manos@engr.wisc.edu

Abstract: Periodic, self-consistent, density functional theory calculations have been performed to demonstrate that subsurface oxygen ($O_{(sb)}$) dramatically increases the reactivity of the Ag(111) surface. $O_{(sb)}$ greatly facilitates the dissociation of H_2, O_2, and NO and enhances the binding of H, C, N, O, O_2, CO, NO, C_2H_2, and C_2H_4 on the Ag(111) surface. This effect originates from an $O_{(sb)}$-induced upshift of the d-band center of the Ag surface and becomes more pronounced at higher $O_{(sb)}$ coverage. Our findings point to the important role that near-surface impurities, such as $O_{(sb)}$, can play in determining the thermochemistry and kinetics of elementary steps catalyzed by transition metal surfaces.

Introduction

It is well-known that small atoms can diffuse into the lattices of transition metals in appreciable quantities, affecting bulk properties and causing various macroscopic phenomena, such as corrosion and embrittlement.[1] When these impurities reside in interstices near the surface, they may directly affect surface properties. The importance of such "subsurface" species has long been speculated upon. A recent STM study of the Pd(111) surface by Rose et al. suggests that subsurface carbon and oxygen are probably common,[2] and studies of H in Ni(111) point to the unique reactivity of subsurface H for the hydrogenation of surface species.[3−5]

Subsurface oxygen ($O_{(sb)}$) is an entirely different species from oxygen adsorbed on the surface ($O_{(a)}$). It has been invoked to explain both modified adsorption behaviors of H and CO[6] and kinetic oscillation phenomena observed in reaction systems, including CO and H_2 oxidation on Pt and Rh surfaces.[7,8] There is even indirect evidence that $O_{(sb)}$ facilitates O_2 dissociation.[2] Furthermore, $O_{(sb)}$ may be viewed as the initial stage in the corrosion and the growth of metal oxides.[9]

The rich interaction between oxygen and Ag[10,11] makes Ag one of the best partial oxidation catalysts for industrial reactions, including the oxidative coupling of methane,[12] partial dehydrogenation of methanol to formaldehyde,[13] and epoxidation of ethylene.[14] Consequently, the oxygen−silver system has been studied extensively, experimentally as well as theoretically.[15−21] The oxidative coupling of methane can achieve high selectivity to C_2 products over CO and CO_2 after an induction period. A Lewis basic oxygen species intercalated in the near-surface region is proposed to be the catalytically active center.[12] For ethylene epoxidation, it has been suggested that $O_{(sb)}$ modifies the electronic properties of the $O_{(a)}$ atoms in its vicinity so that the latter become more vulnerable to attack by the ethylene C=C bond.[15,22] More recently, it has been proposed that a substoichiometric surface oxide is the catalytically active phase[17,21] and that the epoxidation reaction proceeds via an oxametallacycle intermediate.[20,23−26] The interaction between $O_{(sb)}$ and transition metals, particularly Ag, is therefore technologically important and needs to be elucidated. In this contribution, we demonstrate, with a series of density functional theory (DFT) calculations, the dramatic effect of $O_{(sb)}$ on the reactivity of the Ag(111) surface, in particular, how $O_{(sb)}$

(1) Wert, C. A. Trapping of Hydrogen in Metals. In *Hydrogen in Metals II*; Alefeld, G., Völkl, J., Eds.; Springer-Verlag: Berlin, 1978; Vol. 29.
(2) Rose, M. K.; Borg, A.; Mitsui, T.; Ogletree, D. F.; Salmeron, M. *J. Chem. Phys.* **2001**, *115*, 10927.
(3) Ceyer, S. T. *Acc. Chem. Res.* **2001**, *34*, 737.
(4) Greeley, J.; Mavrikakis, M. *Surf. Sci.* **2003**, *540*, 215.
(5) Greeley, J.; Krekelberg, W. P.; Mavrikakis, M. *Angew. Chem., Int. Ed.* **2004**, *43*, 4296.
(6) McCabe, R. W.; Schmidt, L. D. *Surf. Sci.* **1977**, *65*, 189.
(7) Rotermund, H. H.; Pollmann, M.; Kevrekidis, I. G. *Chaos* **2002**, *12*, 157.
(8) Monine, M.; Pismen, L.; Bar, M.; Or-Guil, M. *J. Chem. Phys.* **2002**, *117*, 4473.
(9) Over, H.; Seitsonen, A. P. *Science* **2002**, *297*, 2003.
(10) Pettinger, B.; Bao, X.; Wilcock, I.; Muhler, M.; Schlögl, R.; Ertl, G. *Angew. Chem., Int. Ed.* **1994**, *33*, 85.
(11) Nagy, A. J.; Mestl, G.; Herein, D.; Weinberg, G.; Kitzelmann, E.; Schlögl, R. *J. Catal.* **1999**, *182*, 417.
(12) Nagy, A. J.; Mestl, G.; Schlögl, R. *J. Catal.* **1999**, *188*, 58.
(13) Andreasen, A.; Lynggaard, H.; Stegelmann, C.; Stoltze, P. *Surf. Sci.* **2003**, *544*, 5.
(14) Van Santen, R. A.; Kuipers, H. P. C. E. *Adv. Catal.* **1987**, *35*, 265.
(15) Van den Hoek, P. J.; Baerends, E. J.; van Santen, R. A. *J. Phys. Chem.* **1989**, *93*, 6469.
(16) Li, W.-X.; Stampfl, C.; Scheffler, M. *Phys. Rev. B* **2003**, *67*, 045408.
(17) Li, W.-X.; Stampfl, C.; Scheffler, M. *Phys. Rev. Lett.* **2003**, *90*, 256102.
(18) Gajdos, M.; Eichler, A.; Hafner, J. *Surf. Sci.* **2003**, *531*, 272.
(19) Kokalj, A.; Dal Corso, A.; de Gironcoli, S.; Baroni, S. *Surf. Sci.* **2003**, *532*, 191.
(20) Linic, S.; Barteau, M. A. *J. Am. Chem. Soc.* **2003**, *125*, 4034.
(21) Michaelides, A.; Bocquet, M.-L.; Sautet, P.; Alavi, A.; King, D. A. *Chem. Phys. Lett.* **2003**, *367*, 344.
(22) Moulijn, J. A.; Ponec, V. Heterogeneous Catalysis. In *Catalysis: An Integrated Approach to Homogeneous, Heterogeneous and Industrial Catalysis*; Moulijn, J. A., van Leeuwen, P. W. N. M., van Santen, R. A., Eds.; Elsevier: Amsterdam, 1993.
(23) Jones, G. S.; Mavrikakis, M.; Barteau, M. A.; Vohs, J. M. *J. Am. Chem. Soc.* **1998**, *120*, 3196.
(24) Medlin, J. W.; Barteau, M. A. *J. Phys. Chem. B* **2001**, *105*, 10054.
(25) Linic, S.; Barteau, M. A. *J. Catal.* **2003**, *214*, 200.
(26) Bocquet, M.-L.; Michaelides, A.; Loffreda, D.; Sautet, P.; Alavi, A.; King, D. A. *J. Am. Chem. Soc.* **2003**, *125*, 5620.

modifies both the adsorption of some common adsorbates, including H, C, N, O, O_2, CO, NO, C_2H_2, and C_2H_4, and the dissociation of H_2, O_2, and NO.

Methods

The spin-polarized DFT calculations are performed using DACAPO.[27,28] The exchange-correlation energy and potential are described by the generalized gradient approximation (GGA-PW91).[29,30] Although other GGA exchange-correlation functionals have been developed since the advent of PW91,[27,31,32] there has been no evidence, so far, that any one of them always gives more accurate results for surface adsorption systems than the rest.[33,34] To be consistent with our previous reports, only self-consistently calculated PW91 results will be reported below. The energies of the PW91-optimized structures are also recalculated using the RPBE98 functional.[27] In agreement with previous findings,[27,35] RPBE98 yields increased binding energies (less negative, corresponding to weaker binding) for all the adsorbates studied. Because atomic and molecular species are affected to different extents, the RPBE98 activation energies also differ from their PW91 counterparts, with the former generally being larger by ~0.2 eV.

The ionic cores are described by ultrasoft pseudopotentials,[36] and the Kohn−Sham (KS) valence states are expanded in a plane-wave basis set cut off at 340 eV. The electron density is determined by iterative diagonalization of the KS Hamiltonian, Fermi population of the KS states ($k_BT = 0.1$ eV), and Pulay mixing of the resultant electronic density.[37] Total energies are then extrapolated to $k_BT = 0$ eV.[38] For reference, the calculated PW91 equilibrium lattice constant of Ag is 4.14 Å, in good agreement with the experimentally measured 4.09 Å.[39] The calculated gas-phase H_2, O_2, and NO bond energies are −4.57, −5.64, and −6.73 eV, and the corresponding experimental values are −4.48, −5.12, and −6.51 eV, respectively.[40]

The Ag surface is represented by a four-layer Ag(111) slab constructed from a (2 × 2) unit cell repeated in all three directions. Successive slabs in the *z* direction are separated by a vacuum equivalent to six Ag(111) layers, or ~14 Å. The top two layers of the slab are relaxed. We calculated 1/4 and 1 monolayer (ML) of $O_{(sb)}$ on a five-layer slab with the top three layers relaxed, and we found the vertical displacement of the second-layer Ag atoms from their bulk positions to be negligible and the difference in binding energy compared to the corresponding four-layer results to be within the accuracy of our calculations (see below) in both cases. Thus, the four-layer slab model is sufficient. Adsorption is allowed on the relaxed side of the slab only, with the electrostatic potential adjusted accordingly.[41] The surface Brillouin zone is sampled at 18 special Chadi−Cohen *k*-points.

The binding energy of an adsorbed atom or molecule is calculated as $E_b = E_{total} - E_{slab} - E_{adsorbate(g)}$, that is, with respect to the adsorbate in the gas phase and the metal slab at infinite separation. E_{total}, E_{slab}, and $E_{adsorbate(g)}$ are, respectively, the total energies of the relaxed adsorbate−substrate system, the relaxed clean Ag slab, and the adsorbate in the gas phase. When $O_{(sb)}$ is present, the reference slab includes the $O_{(sb)}$ atoms. The binding energies are verified to converge within 0.05 eV with respect to the *k*-point sampling density and slab thickness. Unless otherwise specified, zero point energies are not included.

The minimum-energy dissociation pathways are determined using the climbing-image nudged elastic band (cNEB) method. This method is designed to rigorously locate the highest saddle point on the minimum-energy path for a given elementary reaction step.[42] The vibrational frequencies of the initial and transition states are calculated in the harmonic approximation. The second derivatives of the energy are determined using a finite-difference approximation and used to construct the mass-weighted Hessian matrix, which is then diagonalized to give the vibrational frequencies.[4] The frequencies are used to verify the transition states and to calculate the pre-exponential factor of the rate constant for each elementary reaction step.[42] Each of the transition states reported below is verified to possess a single vibrational mode with negative curvature in the direction of the reaction coordinate.

Before closing this section, we note that an O/Ag surface phase diagram has been constructed based on our results for the energetics of 0, 1/4, 1/2, and 1 ML of adsorbed O on Ag(111).[43] Our phase diagram is qualitatively consistent with analogous diagrams published by other authors,[17,21] but since this is not directly connected to the main message of the present contribution, it is not included here for the sake of brevity.

Results and Discussion

The binding energies of H, C, N, O, O_2, CO, NO, C_2H_2, and C_2H_4 on Ag(111) are calculated when 0, 1/4, 1/2, and 1 ML of $O_{(sb)}$ are present. In real catalytic systems, coverages of 1/2 and 1 ML of $O_{(sb)}$ may be unrealistically high, although the possibility cannot be excluded that dense $O_{(sb)}$ phases exist on a local scale, that is, in small $O_{(sb)}$ patches or under a more oxidizing chemical environment. In the framework of our model system studies, we choose these specific $O_{(sb)}$ coverages only to demonstrate the trends in the binding energy of adsorbates as a function of $O_{(sb)}$ coverage. The $O_{(sb)}$ atoms are initially located in the octahedral sites, which, as our calculations indicate, are energetically the most favorable sites for pure $O_{(sb)}$ phases at all coverages up to 1 ML. Table 1 shows the calculated binding energies as well as the experimentally determined binding energies on Ag(111), where available.[44−47] Given the uncertainties in the experimental estimates, the calculated binding energies on clean Ag(111) are generally in agreement with them. Atomic and molecular adsorption tends to be more exothermic (binding energy decreases or becomes more negative) in the presence of $O_{(sb)}$ than on the clean surface. This agrees with the finding by Kokalj et al. that $O_{(sb)}$ enhances ethylene adsorption on Ag(001).[19] Li et al. have demonstrated that $O_{(sb)}$ can enhance the adsorption of $O_{(a)}$ on Ag(111), and that the effect is different on different surface adsorption sites depending on their positions relative to the $O_{(sb)}$ atoms,[16] a phenomenon that is also observed in our study.

As the $O_{(sb)}$ coverage increases, the adsorption of these surface species becomes more exothermic. The large effect on the binding energy calculated for some of the molecular species at high $O_{(sb)}$ coverages is accompanied by significant adsorbate-

(27) Hammer, B.; Hansen, L. B.; Nørskov, J. K. *Phys. Rev. B* **1999**, *59*, 7413.
(28) Greeley, J.; Nørskov, J. K.; Mavrikakis, M. *Annu. Rev. Phys. Chem.* **2002**, *53*, 319.
(29) Perdew, J. P.; Chevary, J. A.; Vosko, S. H.; Jackson, K. A.; Pederson, M. R.; Singh, D. J.; Fiolhais, C. *Phys. Rev. B* **1992**, *46*, 6671.
(30) White, J. A.; Bird, D. M. *Phys. Rev. B* **1994**, *50*, 4954.
(31) Perdew, J. P.; Burke, K.; Ernzerhof, M. *Phys. Rev. Lett.* **1996**, *77*, 3865.
(32) Zhang, Y.; Yang, W. *Phys. Rev. Lett.* **1998**, *80*, 890.
(33) Sljivancanin, Z.; Hammer, B. *Surf. Sci.* **2002**, *515*, 235.
(34) Gajdos, M.; Eichler, A.; Hafner, J. *J. Phys.: Condens. Matter* **2004**, *16*, 1141.
(35) Mavrikakis, M.; Rempel, J.; Greeley, J.; Hansen, L. B.; Norskov, J. K. *J. Chem. Phys.* **2002**, *117*, 6737.
(36) Vanderbilt, D. *Phys. Rev. B* **1990**, *41*, 7892.
(37) Kresse, G.; Furthmüller, J. *Comput. Mater. Sci.* **1996**, *6*, 15.
(38) Gillan, M. J. *J. Phys.: Condens. Matter* **1989**, *1*, 689.
(39) Ashcroft, N. W.; Mermin, N. D. *Solid State Physics*; Saunders College: Orlando, FL, 1976.
(40) NIST Computational Chemistry Comparison and Benchmark Database, NIST Standard Reference Database Number 101; Release 10 ed.; Johnson III, R. D., Ed., 2004.
(41) Neugebauer, J.; Scheffler, M. *Phys. Rev. B* **1992**, *46*, 16067.
(42) Henkelman, G.; Uberuaga, B. P.; Jónsson, H. *J. Chem. Phys.* **2000**, *113*, 9901.
(43) Greeley, J.; Mavrikakis, M. In preparation.
(44) Campbell, C. T. *Surf. Sci.* **1985**, *157*, 43.
(45) McElhiney, G.; Papp, H.; Pritchard, J. *Surf. Sci.* **1976**, *54*, 617.
(46) Behm, R. J.; Brundle, C. R. *J. Vac. Sci. Technol. A* **1984**, *2*, 1040.
(47) Stacchiola, D.; Wu, G.; Kaltchev, M.; Tysoe, W. T. *Surf. Sci.* **2001**, *486*, 9.

Table 1. Calculated Binding Energy (B. E., in eV), Magnetic Moment (μ_m, in μ_B), and Geometry of the Most Stable State of the Various Surface Adsorbates on Ag(111) at a Coverage of 1/4 ML as a Function of $O_{(sb)}$ Coverage[a]

	$O_{(sb)}$ coverage												
	0 ML			1/4 ML			1/2 ML			1 ML			
adsorbate	B.E.	μ_m	geometry	B. E.	μ_m	geometry	B. E.	μ_m	geometry	B. E.	μ_m	geometry	Exp.
H	−2.08	0	f	−2.35	0	hβ	−2.70	0	hβ	−3.00	0	h	
C	−3.29	0	f	−3.89	0	hβ	−3.84	0	hβ	−4.27	0.1	h	
N	−2.00	0	f	−2.84	0	hβ	−2.68	0	hβ	−2.79	0.1	h	
O	−3.28	0	f	−3.82	0	hβ	−4.07	0	hβ	−3.97	0.1	h	−3.5[d]
O_2	−0.17	1.0	di-σ/Ot-b-Ot	−0.21	0.8	di-σ/Ot-fβ-Ob	−0.36	0.2	di-σ/Ot-fβ-Ob	−1.12	0.7	di-σ/Ot-*b*-Ot[b,c]	−0.4[d]
CO	−0.29	0	perp/t	−0.55	0	perp/tα[b]	−0.97	0	perp/tβ[b]	−1.10	0	perp/h	>−0.28[e]
NO	−0.42	0.7	perp/f	−0.34	0	perp/hβ	−0.69	0	perp/hβ	−1.21	0.1	perp/h	−0.26[f]
C_2H_2	−0.04	0	flat-η^1/(C,C)t	−0.41	0	cis-η^2/Cb-hβ-Cb	−1.08	0	cis-η^2/Cb-hα-Ct	−1.14	0.4	cis-η^2/Cb-h-Cb	
C_2H_4	−0.11	0	flat-η^1/(C,C)t	−0.21	0	flat-η^1/(C,C)tα[b]	−0.49	0	flat-η^1/(C,C)tβ[b]	−2.82	0	flat-η^1/(C,C)t[b,c]	>−0.4[g]

[a] μ_m is the magnetic moment on the adsorbate only. Experimental estimates of binding energies (Exp.) on clean Ag(111) (i.e., 0 ML of $O_{(sb)}$) are included where available. Abbreviations: t, b, h, f, α, and β, see Figure 1; perp = perpendicular; flat = molecule lies in a plane parallel to the surface; cis = H and surface on opposite sides of the C−C bond. The meaning of the notations: di-σ/Ot-b-Ot = di-σ O_2 state with each O bound to the top of a Ag atom; perp/t = perpendicularly adsorbed to the top of a Ag atom; η^1/(C,C)t = two C atoms bound to the top of the same Ag atom; η^2/Cb-h-Cb = two C atoms bound to two adjacent bridge sites over an hcp site. [b] Sky hook effect, in which the surface adsorbate pulls the contacting Ag atom up from the surface by 0.5−1.5 Å. [c] Substantial surface reconstruction. [d] From ref 44. [e] From ref 45. Value is initial heat of adsorption. [f] From ref 46. [g] From ref 47. Value is based on desorption barrier and becomes −0.5 eV with 0.1 ML of coadsorbed surface oxygen.

Table 2. Calculated Activation Energies (E_a), Pre-exponential Factors (Γ), and Forward Rate Constants; ($k = \Gamma \times \exp(-E_a^{ZPE}/k_B T)$) for the Dissociation of H_2, O_2, and NO on Ag(111) with 0 and 1/2 ML of $O_{(sb)}$ at 300 and 550 K

reaction	$O_{(sb)}$ coverage	E_a (eV)	ZPE-corrected E_a^{ZPE} (eV)	Γ (s^{-1}) (T = 300 K)	k (s^{-1}) (T = 300 K)	Γ (s^{-1}) (T = 550 K)	k (s^{-1}) (T = 550 K)
$H_2 \rightarrow 2H$	0	1.11	1.04	6.71×10^8	2.03×10^{-9}	1.02×10^8	2.85×10^{-2}
	1/2	0.74	0.72	1.32×10^8	1.17×10^{-4}	3.72×10^7	9.92×10^0
$O_2 \rightarrow 2O$	0	1.11	1.06	7.47×10^{12}	1.01×10^{-5}	4.17×10^{12}	7.49×10^2
	1/2	0.90	0.86	2.72×10^{13}	1.07×10^{-1}	1.96×10^{13}	2.72×10^5
$NO \rightarrow N + O$	0	3.12	3.08	1.13×10^{12}	2.23×10^{-40}	4.74×10^{11}	2.97×10^{-17}
	1/2	2.38	2.33	2.16×10^{12}	1.43×10^{-27}	9.41×10^{11}	4.02×10^{-10}

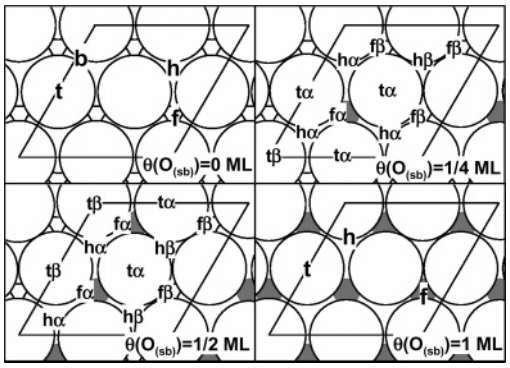

Figure 1. Top-view schematics identifying adsorption sites on the Ag(111) surface at different $O_{(sb)}$ coverages ($\theta(O_{(sb)})$) as indicated in each panel; 0 ML refers to a surface without $O_{(sb)}$. The abbreviations are: t = top; b = bridge; h = hcp; f = fcc. Large open circles represent Ag atoms, and small gray circles represent O atoms. The surface unit cells are outlined.

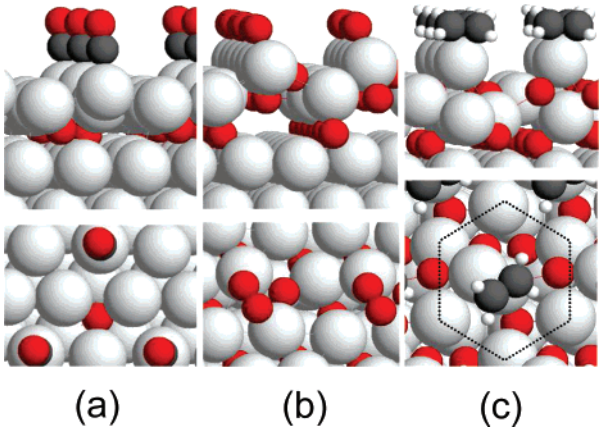

Figure 2. Side (upper panel) and top (lower panel) views of: (a) $CO_{(a)}$ with 1/2 ML of $O_{(sb)}$; (b) $O_{2(a)}$ with 1 ML of $O_{(sb)}$; (c) $C_2H_{4(a)}$ with 1 ML of $O_{(sb)}$. Large silver spheres represent Ag atoms; medium red spheres represent O atoms; medium gray spheres represent C atoms; and small white spheres represent H atoms. The dashed lines in (c) outline a structure similar to the $p(4 \times 4)-Ag_{1.8}O$ phase. Coverage of surface adsorbates is 1/4 ML.

induced surface reconstruction and movement of $O_{(sb)}$ atoms. For instance, in the presence of 1/4 and 1/2 ML of $O_{(sb)}$, CO pulls the contacting Ag atom up by 1.1 and 0.6 Å from the surface, respectively (see Figure 2a), an example of the "sky hook" effect.[48,49] In the case of O_2 with 1 ML of $O_{(sb)}$, the top Ag layer buckles to form an oxide-like O−Ag−O trilayer structure (see Figure 2b). When coadsorbed with 1 ML of $O_{(sb)}$, the C_2H_4 molecule pulls a Ag atom completely out of the surface, and the remaining Ag atoms of the surface layer, together with the $O_{(sb)}$ atoms, relax into a structure (see Figure 2c) akin to the previously reported $p(4 \times 4)-Ag_{1.8}O$ phase.[21,50]

Even more significant is the finding that $O_{(sb)}$ enhances the kinetics of H_2, O_2, and NO dissociation on Ag(111). Figure 3 summarizes the results for H_2, O_2, and NO dissociation at 0 and 1/2 ML of $O_{(sb)}$. Complete minimum-energy paths have been calculated, but for brevity, only the binding energy levels of the initial, transition, and final states are shown. Sample reaction kinetic parameters are tabulated in Table 2. It can be seen that

(48) Horch, S.; Lorensen, H. T.; Helveg, S.; Lægsgaard, E.; Stensgaard, I.; Jacobsen, K. W.; Nørskov, J. K.; Besenbacher, F. *Nature* **1999**, *398*, 134.
(49) Greeley, J.; Gokhale, A. A.; Kreuser, J.; Dumesic, J. A.; Topsøe, H.; Topsøe, N. Y.; Mavrikakis, M. *J. Catal.* **2003**, *213*, 63.
(50) Bocquet, M.-L.; Sautet, P.; Cerda, J.; Carlisle, C. I.; Webb, M. J.; King, D. A. *J. Am. Chem. Soc.* **2003**, *125*, 3119.

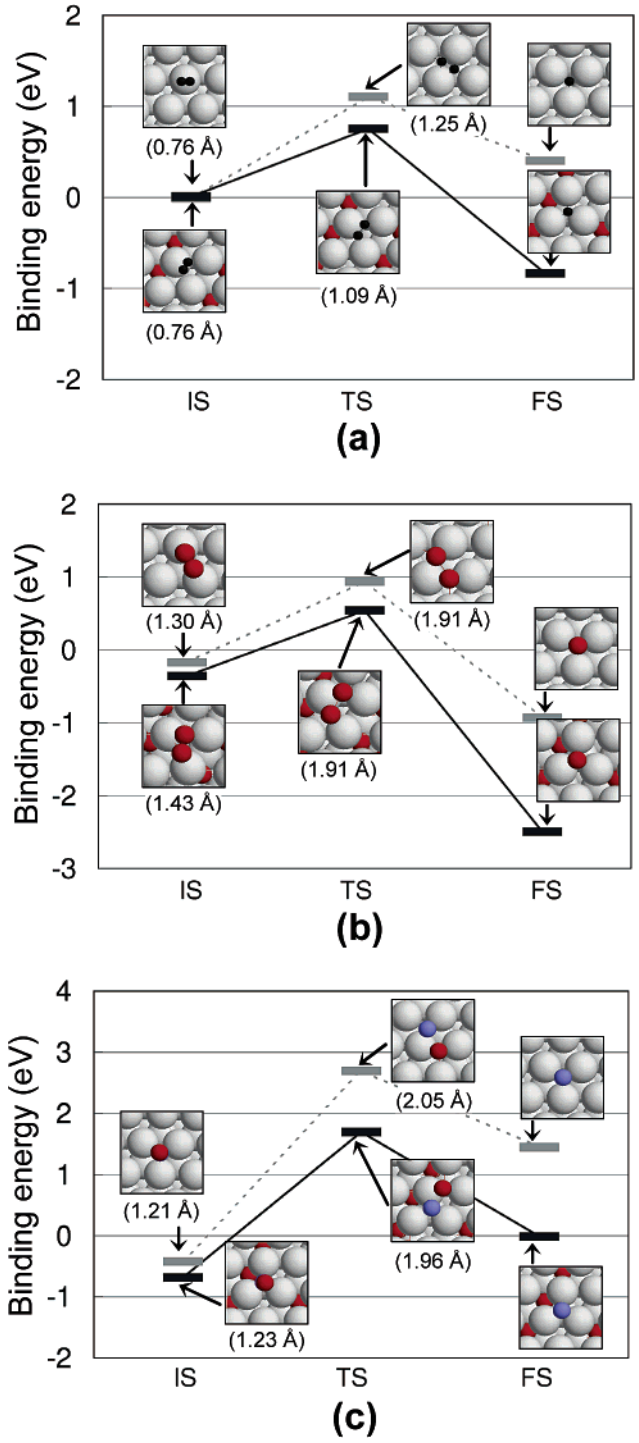

Figure 3. Summary of (a) H_2, (b) O_2, and (c) NO dissociation on Ag(111). The binding energies and snapshots of the initial (IS), transition (TS), and final (FS) states of each reaction are shown. Dashed (continuous) lines give the energy profiles on Ag(111) with 0 ML (1/2 ML) of $O_{(sb)}$. The zero of the energy axis corresponds to the total energy of the adsorbate molecule in the gas phase and the corresponding Ag slab at infinite separation. Large silver spheres represent Ag atoms; medium red spheres represent O atoms; medium blue spheres represent N atoms; and small black spheres represent H atoms. The molecular initial states of $O_{2(a)}$ and $NO_{(a)}$ are those listed in Table 1. For H_2 dissociation, the initial states are essentially gas-phase H_2. The energy of each final state is calculated as the sum of the atomic products at 1/4 ML (therefore only one product atom is shown) with respect to the gas-phase molecule (e.g., $E_b^N + E_b^O -$ bond energy$(NO_{(g)})$ gives the energy of the final state of NO dissociation). The numbers below the snapshots indicate the length of the intramolecular bond. For reference, the gas-phase H_2, O_2, and NO bond lengths are 0.74, 1.21, and 1.15 Å (experimental[55]) and 0.75, 1.24, and 1.18 Å (calculated), respectively.

Table 3. Average Center (ϵ_d) and Spread (σ) of the d-Band of the Ag(111) Surface at Different $O_{(sb)}$ Coverages: ϵ_d Values in Bold are used in Figure 4

		0 ML	1/4 ML	1/2 ML	1 ML
slab with $O_{(sb)}$	ϵ_d (eV)	**−4.10**	**−4.01**	**−3.57**	**−3.25**
	σ	3.13	3.59	3.71	4.03
slab with $O_{(sb)}$ removed	ϵ_d (eV)	−4.10	−3.87	−3.71	−3.60
	σ	3.13	2.98	2.80	2.60

the dissociation products, namely, atomic H, O, and N, are stabilized by $O_{(sb)}$ to a much greater extent than the respective molecular initial states. The transition states, being located between the initial and final states, are stabilized to an intermediate extent. The different $O_{(sb)}$-induced stabilization experienced by the transition and molecular states results in markedly reduced reaction barriers (by 0.37, 0.21, and 0.73 eV for H_2, O_2, and NO dissociation, respectively), which translates into substantially higher reaction rates (see Table 2). The increase in the reaction rates, with respect to those on the clean Ag surface, is on the order of 10^4 ($T = 300$ K) and 10^2 ($T = 550$ K; actual catalytic partial oxidation temperature[51]) for H_2 and O_2 dissociation but is much greater for NO dissociation because the rate for NO dissociation is vanishingly small on clean Ag(111). These findings are in accord with the general trend established previously for the dissociation of diatomic molecules on transition metal surfaces, which suggests that surfaces that bind dissociation products more strongly are characterized by smaller dissociation barriers.[52−54] We note here that O_2 dissociation has been recently identified as one of the rate-controlling steps in C_2H_4 epoxidation on Ag.[25] Our finding that subsurface oxygen facilitates the kinetics of O_2 dissociation suggests that $O_{(sb)}$ might play an important role in ethylene epoxidation catalysis.

To see how $O_{(sb)}$ modifies the properties of the Ag(111) surface, we calculate the surface d-band center (ϵ_d), as proposed in the Hammer−Nørskov model, to characterize surface reactivity at different coverages of $O_{(sb)}$.[28,56] The DACAPO code calculates the density of states as projected onto each atom. As a first-order approximation, the ϵ_d of the average surface d-band is equal to the average of the ϵ_d of each surface Ag atom. For heterogeneous surfaces (i.e., $O_{(sb)}$ coverage other than 0 and 1 ML), we have calculated the arithmetic average of the ϵ_d's of the Ag atoms in the surface unit cell, as has been done before.[54,57] More specifically, we have calculated the average ϵ_d and the average spread (σ) of the surface d-band at different $O_{(sb)}$ coverages, for both the Ag(111) surface loaded with $O_{(sb)}$ and the same surface, frozen, with the $O_{(sb)}$ removed. The results are listed in Table 3. The binding energies of H, C, N, O, CO, NO, and C_2H_2 are plotted against the calculated ϵ_d in Figure 4. O_2 and C_2H_4 cause substantial surface reconstruction in the presence of 1 ML of $O_{(sb)}$ and are not included.

(51) Berty, J. M. *Appl. Ind. Catal.* **1983**, *1*, 207.
(52) Nørskov, J. K.; Bligaard, T.; Logadottir, A.; Bahn, S.; Hansen, L. B.; Bollinger, M.; Bengaard, H.; Hammer, B.; Sljivancanin, Z.; Mavrikakis, M.; Xu, Y.; Dahl, S.; Jacobsen, C. J. H. *J. Catal.* **2002**, *209*, 275.
(53) Michaelides, A.; Liu, Z. P.; Zhang, C. J.; Alavi, A.; King, D. A.; Hu, P. *J. Am. Chem. Soc.* **2003**, *125*, 3704.
(54) Xu, Y.; Ruban, A. V.; Mavrikakis, M. *J. Am. Chem. Soc.* **2004**, *126*, 4717.
(55) *CRC Handbook of Chemistry and Physics*, 85th ed.; CRC Press: Boca Raton, FL, 2004.
(56) Hammer, B.; Nørskov, J. K. Theory of Adsorption and Surface Reactions. In *Chemisorption and Reactivity on Supported Clusters and Thin Films*; Lambert, R. M., Pacchioni, G., Eds.; Kluwer Academic Publishers: Dordrecht, The Netherlands, 1997; p 285.
(57) Pallassana, V.; Neurock, M.; Hansen, L. B.; Nørskov, J. K. *J. Chem. Phys.* **2000**, *112*, 5435.

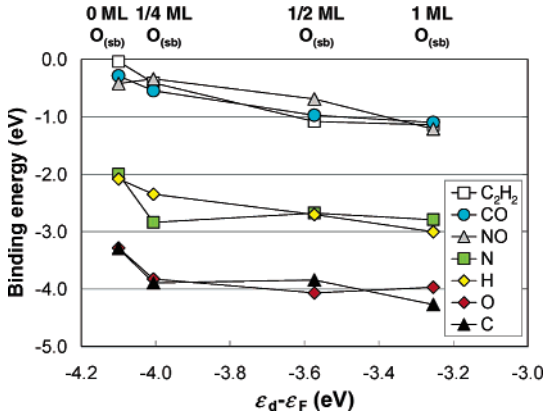

Figure 4. The binding energies of H, C, N, O, CO, NO, and C_2H_2 plotted against the d-band center (ϵ_d) of the clean Ag(111) surface (without surface adsorbates) at different $O_{(sb)}$ coverage. The ϵ_d values here are those shown in bold in Table 3.

The data in Table 3 show that, as a result of the interplay among various geometric ($O_{(sb)}$-induced strain, etc.) and electronic (coupling to $O_{(sb)}$, etc.) effects, a consistent upshift of the ϵ_d is observed. The binding energies correlate fairly well with the ϵ_d; as the coverage of $O_{(sb)}$ increases, the ϵ_d shifts toward the Fermi level, and the absolute magnitude of the binding energies of the surface adsorbates tends to increase. This trend agrees with previous findings,[58] suggesting that the Hammer–Nørskov model can explain the changes in the reactivity of metal surfaces caused by $O_{(sb)}$. We note that the effect of $O_{(sb)}$ on the binding energies of the atomic species is most pronounced at low $O_{(sb)}$ coverage. At higher $O_{(sb)}$ coverage, the effect of $O_{(sb)}$ seems to reach saturation at least for some of the adsorbates considered. For instance, the binding energies of N and O show little further change when the $O_{(sb)}$ coverage increases beyond 1/4 ML.

We note in passing that charge transfer from Ag to $O_{(sb)}$ will also tend to generate negatively charged $O_{(sb)}$, which would, in turn, enhance the dipole generated by alkali atoms adsorbed on the Ag surface, thereby further enhancing the promoting effect that alkali elements have been shown to have on ethylene epoxidation on Ag.[59]

To gain further insight, we compare the electronic structure of O_2 and NO on Ag(111) at 0 and 1/2 ML of $O_{(sb)}$ in Figure 5.[60] Upon adsorption, there are donation and back-donation of charge density between the adsorbate and the surface, as well as internal charge density redistribution (first image of each panel). These processes are manifested in the depletion of the bonding orbitals, namely, the π of O_2 and the 5σ, and probably the 4σ and 1π,[34] of NO, and in the enhancement of the antibonding π^* orbital of O_2 and $2\pi^*$ orbital of NO. In the presence of $O_{(sb)}$, the respective loss and gain are intensified (second image of each panel), indicating enhanced coupling between the surface and adsorbate states and a weakened intramolecular bond. This observation is in agreement with the Hammer–Nørskov model, which suggests that an upshifted ϵ_d leads to stronger interaction of the d-band with a high-lying antibonding adsorbate state, thus causing the adsorbate to adsorb more strongly.[61]

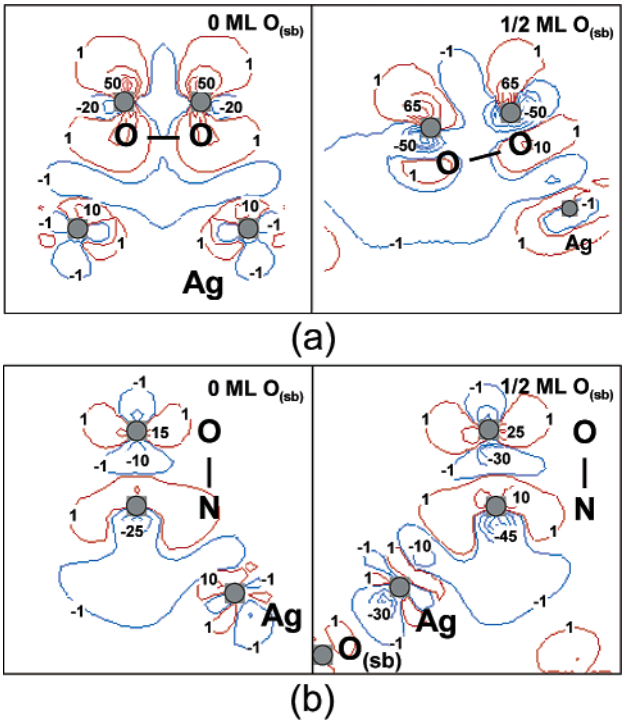

Figure 5. Electron density difference (Δn) contours for 1/4 ML of (a) $O_{2(a)}$ and (b) $NO_{(a)}$ on Ag(111). $\Delta n = n_{total} - n_{slab} - n_{adsorbate}$, where n_{total}, n_{slab}, and $n_{adsorbate}$ are the electron densities of the entire system, the Ag(111) slab with 0 ML (left panels) or 1/2 ML (right panels) of $O_{(sb)}$, and the adsorbate in the gas phase, respectively. The values of the contours are as labeled and have the units of number of electrons per 10^2 Å^3. Blue contours indicate regions of charge density loss, and red contours indicate regions of gain. The adsorbate configurations correspond to the initial states of O_2 and NO dissociation shown in Figure 3. The gray circles indicate the positions of the atoms as labeled. The smaller circle labeled Ag in the right image of panel (a) indicates that the contour plane does not cut through the center of that Ag atom.

Conclusions

Subsurface oxygen ($O_{(sb)}$) increases the reactivity of the Ag(111) surface by inducing an upshift of the surface d-band center. It stabilizes the adsorption of H, C, N, O, O_2, CO, NO, C_2H_2, and C_2H_4 on Ag(111) and enhances the kinetics of H_2, O_2, and NO dissociation substantially. These findings suggest that $O_{(sb)}$ may play an important role in industrial reactions involving Ag and other transition metal catalysts. Furthermore, one could envision using $O_{(sb)}$ and perhaps other near-surface impurities to systematically alter or fine-tune the catalytic properties of transition metal surfaces.

Acknowledgment. This research used EMSF-PNNL, DOE-NERSC, and NPACI computing resources. M.M. acknowledges financial support from a NSF-CAREER award (CTS-0134561) and a DOE-BES Catalysis Science Grant (DE-FG02-03ER15469).

JA043727M

(58) Mavrikakis, M.; Hammer, B.; Nørskov, J. K. *Phys. Rev. Lett.* **1998**, *81*, 2819.
(59) Linic, S.; Barteau, M. A. *J. Am. Chem. Soc.* **2004**, *126*, 8086.
(60) H_2 is not included in Figure 5 because it does not adsorb on the Ag(111) surface, with or without $O_{(sb)}$.
(61) Hammer, B.; Morikawa, Y.; Nørskov, J. K. *Phys. Rev. Lett.* **1996**, *76*, 2141.